

# Development of Highly Spectral-Resolved Charge Exchange Recombination Spectroscopy in Heliotron J

S. Kobayashi<sup>1</sup>, S. Ohshima<sup>1</sup>, S. Kado<sup>2</sup>, H. Y. Lee<sup>3</sup>, T. Minami<sup>4</sup>, T. Kagawa<sup>4</sup>, T. Mizuuchi<sup>1</sup>, K. Nagasaki<sup>1</sup>, S. Yamamoto<sup>1</sup>, H. Okada<sup>1</sup>, T. Minami<sup>1</sup>, S. Murakami<sup>5</sup>, Y. Suzuki<sup>6</sup>, Y. Nakamura<sup>2</sup>, K. Hanatani<sup>1</sup>, S. Konoshima<sup>1</sup>, K. Toshi<sup>1</sup> and F. Sano<sup>1</sup>

<sup>1</sup>*Institute of Advanced Energy, Kyoto University, Uji, Kyoto, 611-0011, Japan*

<sup>2</sup>*School of Engineering, University of Tokyo, Bunkyo, Tokyo, 113-8656, Japan*

<sup>3</sup>*Graduate School of Energy Science, Kyoto University, Uji, Kyoto, 611-0011, Japan*

<sup>4</sup>*Faculty of Engineering, Kyoto University, Uji, Kyoto, 611-0011, Japan*

<sup>5</sup>*Graduate School of Engineering, Kyoto University, Uji, Kyoto, 606-8501, Japan*

<sup>6</sup>*National Institute for Fusion Science, Toki, Gifu, 509-5292, Japan*

(Received: 19 November 2009 / Accepted: 3 February 2010)

In this study, a high spectral-resolved charge exchange recombination spectroscopy (CXRS) has been developed for the Heliotron J plasma aiming at improving the resolution of the rotation velocity, since it is expected that the rotation velocity would be small due to relatively high viscosity of the Heliotron J configuration. A monochromator with Echelle-type grating ( $f=200\text{mm}$ , F2.9) designed specially for the HeII (468.57nm) and CVI (529.05nm) CXR lines has dispersion of 0.163nm/mm for 468.57nm and 0.186nm/mm for 529.05nm, which corresponds to the resolution of the rotation velocity of 1.7 km/s/pix. In order to improve the spatial resolution of the CXRS measurement in the case that the heating neutral beam (NB) is used for the diagnostics, two sets of the viewing chords have been designed; one is for the peripheral CXRS measurement and the other is for the core CXRS. The spatial resolution of the viewing chords has been estimated using a numerical calculation based on the CXR emission model assuming peaked and hollow impurity ion density profiles. The observation area for the peripheral measurement is from  $\rho = 0.4$  to 1.0 for the standard configuration of Heliotron J, with the spatial resolution ( $\Delta\rho$ ) less than  $\pm 0.06$ . The viewing chord for the core CXRS measurement has a spatial resolution of  $\pm 0.05$  at the plasma core.

Keywords: Charge exchange recombination spectroscopy, Echelle-type monochromator, high dispersion relation, numerical calculation of spatial profile of CXR emission

## 1. Introduction

In magnetically confined plasmas, measurement of radial profile of pressure (density times temperature) and toroidal and poloidal rotation velocities ( $v_t$  and  $v_p$ ) is indispensable not only to understand the heat or particle transport but also the control the radial electric field through the force balance. The radial electric field is one of the key factors to reduce the turbulent transport through  $E \times B$  shear flow, which affects appearance of the transport barrier such as high confinement mode (H-mode) [1-3] or internal transport barrier (ITB) [4-6]. In recent tokamak research relevant to burning plasma physics, the control of the rotation velocity is crucial subject to stabilize the resistive wall mode (RWM) and control the edge localized mode (ELM) [7, 8]. To solve the problem, measurement of a high-resolved (spatial, spectral and temporal) rotation velocity is important. The spectroscopy of a line emission from the charge exchange recombination reaction between

impurity ion and neutral particle introduced by neutral beam injection has been utilized for the measurements of the radial profile of the impurity ion temperature, density and rotation velocity in high temperature fusion plasmas [9]. In heliotron/stellarator configurations, however, the rotation velocity in the peripheral region is slower than tokamak (several km/s) because of a relatively high viscosity due to its three-dimensional structure of the magnetic configuration [10]. Therefore, the measurement of the rotation velocity with good resolution is required for the precise estimation of the radial electric field.

In the helical-axis heliotron device Heliotron J ( $R/a = 1.2\text{m}/0.17\text{m}$ ) with  $L/M=1/4$  helical winding coil, H-mode transition has been observed in electron cyclotron heating and neutral beam injection (NBI) plasmas, where  $L$  and  $M$  are the pole number and the helical pitch [11]. It has been found that the appearance of the transition has a dependence on the edge rotational transform which influences on the viscous damping rate [11]. Therefore it is

author's e-mail: kobayashi@iae.kyoto-u.ac.jp

important to study the relation among the radial profile of the rotation velocity, the transition and the viscosity depending on the magnetic configuration. In Heliotron J, both co- and counter NBI systems have been installed, then, the study on the intrinsic rotation and its dependence on the magnetic configuration make a contribution to understand the physics of high temperature torus plasmas.

In this study, we develop a high spectral- and spatial-resolved CXRS system, aiming at obtaining radial profile of  $T_i$  and  $v_i$  in Heliotron J plasmas. We describe the specifications and the measurement result of the linear dispersion for the newly developed monochromator using camera lens and Echelle-type diffraction grating, which is designed to obtain a rotation velocity resolution of 1~2 km/s. In order to achieve good spatial resolution for the peripheral CXRS measurement when the heating neutral beam is used for diagnostic, the sight-lines are designed using numerical calculation based on the result of the neutral beam trajectory analysis using Monte-Carlo method [12]. The sight-lines which observe at the plasma core are proposed using a newly designed viewing port.

## 2. High spectral-resolved monochromator for CXRS measurement in Heliotron J

The high spectral-resolved monochromator specialized in the CXRS measurement for CVI ( $n=8 \rightarrow 7$ , 529.05nm) and HeII ( $n=4 \rightarrow 3$ , 468.57nm) lines is developed. To achieve a compatibility high-spectral resolution and high-efficiency, the monochromator equips one pair of camera lenses with a focal length of 200mm, prism, and Echelle-type diffraction grating (31.6 gr/mm, blaze angle of 71 degree). The effective F number is set to be 2.9 to fit the numerical aperture (NA) of the optical fiber (NA=0.2) at the incident slit. The camera with back-illuminated charge coupled device ( $16\mu\text{m}^2/\text{pix}$ ,  $512 \times 512$  pix) having quantum efficiency more than 0.8 in

the range from 450 nm to 750 nm is mounted on the monochromator.

The linear dispersion is investigated using a monochromator calibrated using hollow-cathode lamps. Figures 1(a) and 1(b) show the obtained spectrum for HeII and CVI lines using another monochromator, respectively. The linear dispersion is 0.163nm/mm ( $=2.60 \times 10^{-3}$  nm/pix) around 468nm and 0.186nm/mm ( $=2.97 \times 10^{-3}$  nm/pix) around 529nm, which corresponds to the 1.7km/s of the rotation velocity of the Doppler-shifted CXR line-emission. The monochromator developed for the CXRS diagnostic

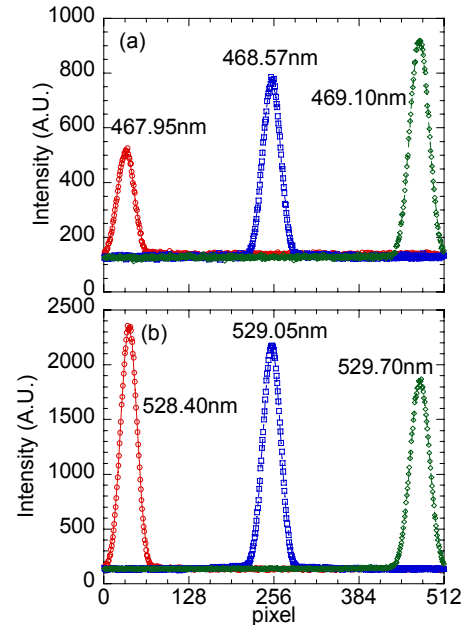


Fig.1 Spectral profile around HeII (468.57nm) and CVI (529.05nm) lines obtained by the Echelle monochromator. The incident light is produced by another monochromator whose wavelength was absolutely calibrated by hollow-cathode lamps

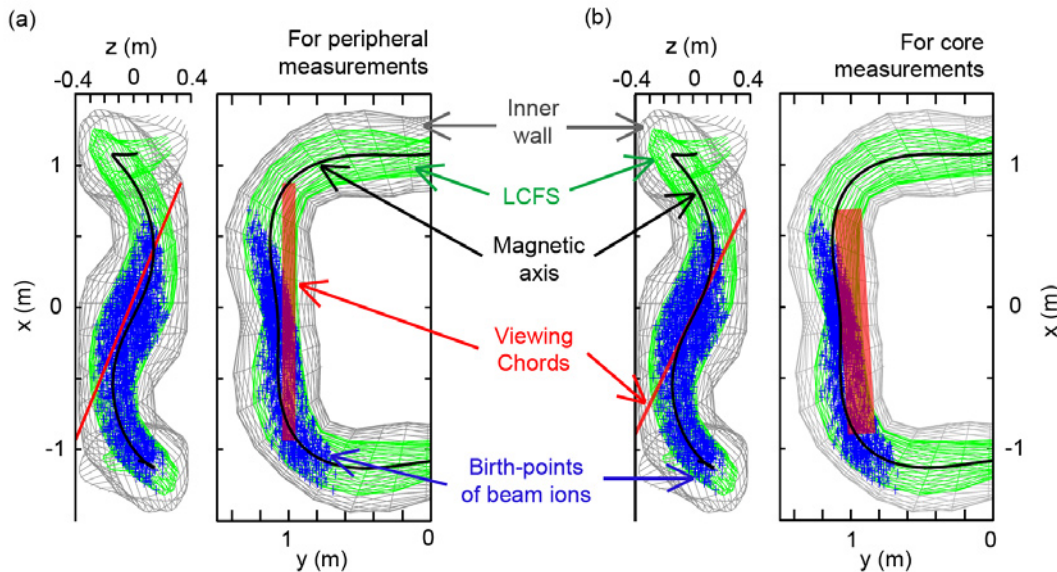


Fig.2 Schematic view of the designed CXRS sight-lines of Heliotron J for (a) peripheral viewing chords from the present viewing port and for (b) core CXRS measurements by a newly designed viewing port.

enables us to measure the rotation velocity precisely with the 1km/s resolution.

### 3. Design of viewing chords and estimation of spatial resolution

To obtain good spatial resolution for CXRS measurement in the case that the neutral beams for plasma heating is used as diagnostics, we designed two sets of toroidally viewing chords; one is for the peripheral region measurement from the present viewing port. The other is for the core plasma measurement from a newly designed viewing port. Figure 2 (a) and (b) show the top and side view of Heliotron J device including the inner vacuum vessel, the last closed flux surface (LCFS) for the standard configuration of Heliotron J, the birth-points of the beam ions deduced by Monte-Carlo method [12] and the designed chords for the peripheral and core CXRS measurements, respectively. The Heliotron J is a helical-axis heliotron configuration and its magnetic axis has a square shape from top view and a sine-like curve from side one. If the sight-lines are chosen parallel to or along with the magnetic axis with taking the region of the neutral beam passing into account, it can minimize the deviation of sight-lines from flux surfaces [13]. The deviation of the sight-lines from the flux surface, i.e. the spatial resolution, is calculated numerically using the three-dimensional equilibrium data and the CXR emission position, which will be described later. The chords shown in Fig. 2 are selected to minimize the spatial resolution deduced by the numerical calculation. As for the peripheral measurements, the twenty chords having a pitch of 5 mm

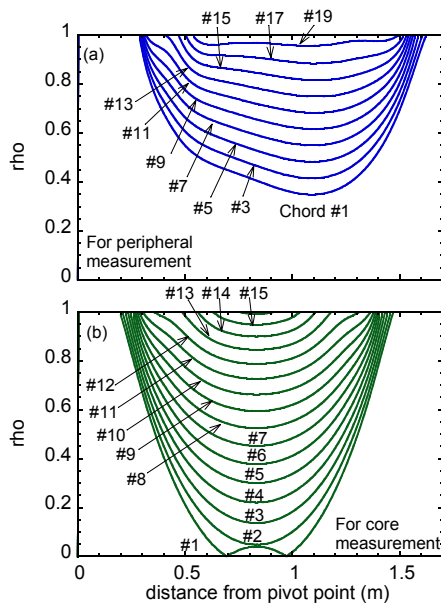


Fig.3 Observation point for two sets of toroidally viewing chords; (a) for the peripheral region measurement and (b) for the core plasma measurement.

are aligned. The chords for core measurements also have twenty chords with 10mm pitch. In this case, the five chords for the inner torus side observe outside LCFS for the standard configuration of Heliotron J, which are used for large volume or inwardly-shifted configurations. Note that the core CXRS chords are set to be symmetrical to the Heliotron J configuration. The optimization method would be applicable to design the sight-lines of spectroscopic measurements related to emission by collision with neutral beam such as CXRS, Beam Emission Spectroscopy (BES) in the helical-axis heliotron/stellarator configurations.

Figure 3(a) and 3(b) show the observation point along each viewing chord as a function of the distance from the pivot point at which the reflection mirror will be equipped. The calculation was done for the standard configuration of Heliotron J. In the case of the peripheral measurement, the observation area varies from  $\rho = 0.3$  to 1, where  $\rho$  is the normalized minor radius, which is limited by the size of the viewing port. On the contrary, the viewing chords for the core plasma measurement can observe from the core to the edge region. The detection length of the edge viewing chords for the peripheral measurement are more than two times longer than that for the core measurement, which implies the peripheral viewing chords are expected to obtain the CXR intensity effectively in the edge region.

To estimate the spatial resolution of the viewing chords, a numerical calculation is carried out. The obtained CXR intensity  $I_{\text{CXR}}$  having a chord  $dl$  can be expressed by the formula,

$$I_{\text{CXR}} \propto \int A_{\text{nm}} n_{\text{imp}} n_{\text{beam}} \sigma_{\text{CXR}} |\nu| d\omega dl, \quad (1)$$

where  $A_{\text{nm}}$ ,  $n_{\text{imp}}$ ,  $n_{\text{beam}}$ ,  $\sigma_{\text{CXR}}$  and  $\nu$  are the transition probability of the line emission, the impurity density, the neutral beam density, the cross section of charge exchange reaction and the relative velocity between beam and

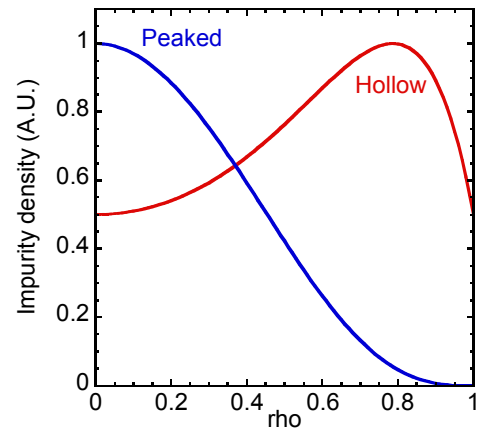


Fig.4 Radial profile of impurity density used in the numerical calculation for the spatial resolution of viewing chords.

impurity ion.  $d\omega$  is the solid angle at the CXR emission. The neutral beam density was estimated by the neutral beam trajectory deduced from the Monte-Carlo simulation of the birth-point analysis for beam ions [12]. The relative velocity is assumed to be the beam velocity because the bulk ion temperature measured by the charge exchange neutral particle analyzer (several hundreds eV) is much smaller than the acceleration voltage of NBI ( $\sim 30$  kV) in Heliotron J plasma [14]. As shown in Fig.4, two radial profiles of the impurity ion density are assumed; the peaked profile is considered to be for the  $C^{6+}$  ion density since the ionization potential of  $C^{6+}$  (490eV) is in the same order of the core electron temperature of Heliotron J. The  $He^{2+}$  ion density profile introduced by additionally Helium gas puffing is assumed to be hollow one because it has lower ionization potential (54.4eV). The diameter of the viewing chords are set to be  $\phi=10$ mm. Figures 5(a) and (b) show the calculated CXR emissivity as a function of the normalized minor radius for the peripheral region measurement in the two cases of impurity ion density profile. The  $1/e$  width and the total emissivity of each profile regard as the spatial resolution and the expected CXR intensity, respectively, which is shown in Table 1. Sight-lines of the viewing chords for peripheral measurement have observation area of  $0.4 < \rho < 1$  with the spatial resolution  $\Delta\rho$  from  $\pm 0.06$  to  $\pm 0.03$ . In the peaked profile case, the CXR intensity decreases as increasing minor radius. In the edge region  $\rho > 0.85$ , it was less than  $1/100$  of that at  $\rho = 0.4$ . For the hollow profile case, on the contrary, the CXR intensity in the edge region ( $\rho > 0.8$ ) is almost same as that for  $\rho = 0.4$ . These results suggest that

the additional Helium gas puffing whose ionization potential is lower than the electron temperature would be effective for the precise estimation of the edge CXRS measurement for Heliotron J. The chords for CXRS measurement can be achieved with good spatial resolution of less than 0.06 even using the heating neutral beam as diagnostic one in the medium-sized experimental device.

Figure 6 (a) and (b) show the radial profile of the calculated CXR emissivity for the core plasma viewing chords under the condition of the peaked and hollow impurity density profiles, respectively. In the case of the peaked density profile, even at the core chord ( $\rho=0$ ), the sight-line has a spatial resolution  $\Delta\rho$  less than  $\pm 0.05$ . However, for the sight-lines of  $\rho = 0.1-0.4$ , spatial resolution  $\Delta\rho$  is slightly higher than  $\pm 0.05$ , since these chords are designed to have the optimum spatial resolution at the plasma core. The CXR intensity becomes smaller as the normalized radius. In the edge region more than  $\rho > 0.8$ , the CXR intensity is 100 times smaller than that at the plasma core. On the contrary, the edge CXR intensity under the case of the hollow density profile shown in Fig. 6 (b) has a significant value the almost same as that at the core region. The edge region more than  $\rho > 0.8$ , the CXR intensity is slightly lower than that for the peripheral viewing chords in Fig. 5, because the core plasma viewing chords designed symmetrically and the path-length of the edge chords for the core CXR measurement is shorter than that for the peripheral viewing chords as shown in Fig. 3. Therefore, the combination of the two sets of viewing chords is effective to observe the core and the edge regions simultaneously.

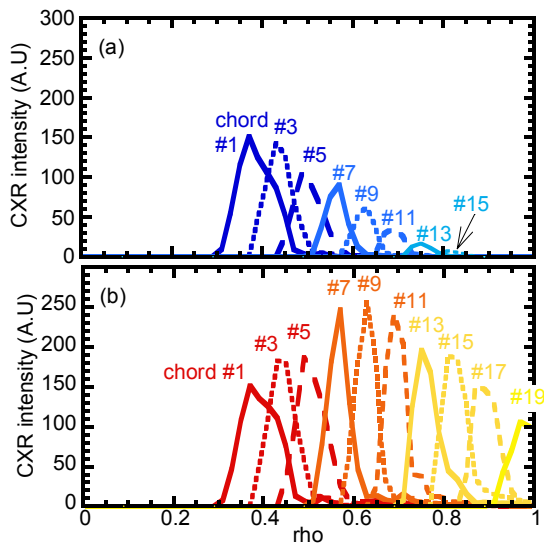


Fig.5 CXR emissivity as a function of the normalized minor radius for the peripheral viewing chords deduced from numerical calculation of CXR emission profile in the cases of (a) peaked and (b) hollow impurity ion density profiles.

#### 4. Summary

We designed a high spectral- and spatial-resolved

Table 1 Observation location and spatial resolution of the peripheral viewing chords in the cases that the peaked and hollow impurity density profiles are assumed.

No.	Peaked profile		Hollow profile	
	$\rho$	$\Delta\rho$	$\rho$	$\Delta\rho$
#1	0.384	$\pm 0.057$	0.391	$\pm 0.060$
#3	0.436	$\pm 0.042$	0.440	$\pm 0.043$
#5	0.499	$\pm 0.043$	0.504	$\pm 0.040$
#7	0.563	$\pm 0.032$	0.566	$\pm 0.033$
#9	0.625	$\pm 0.032$	0.628	$\pm 0.032$
#11	0.689	$\pm 0.031$	0.693	$\pm 0.031$
#13	0.751	$\pm 0.032$	0.758	$\pm 0.037$
#15	0.815	$\pm 0.032$	0.823	$\pm 0.036$
#17	--	--	0.891	$\pm 0.039$
#19	--	--	0.977	$\pm 0.040$

CXRS system for Heliotron J using the heating NBI as the diagnostic beam. An Echelle monochromator ( $f=200\text{mm}$ , F2.9) was specially designed for the HeII (468.57nm) and CVI (529.05nm) CXR measurements. The high dispersion at  $0.163\text{nm/mm}$  ( $=2.60\times 10^{-3}\text{ nm/pix}$ ) for 468nm and  $0.186\text{nm/mm}$  ( $=2.97\times 10^{-3}\text{ nm/pix}$ ) for 529nm can be achieved, which corresponds to the resolution of the rotation velocity by  $1.7\text{km/s/pix}$ . The viewing chords for peripheral and core CXRS measurements were investigated using the numerical calculation. The sight-lines for peripheral measurements have a spatial resolution  $\Delta\rho$  of less than  $\pm 0.06$  in the range of  $0.4 < \rho < 1.0$ . The viewing chord for the core CXRS measurement with a spatial resolution of  $\Delta\rho = \pm 0.05$  was achieved using a newly designed viewing port.

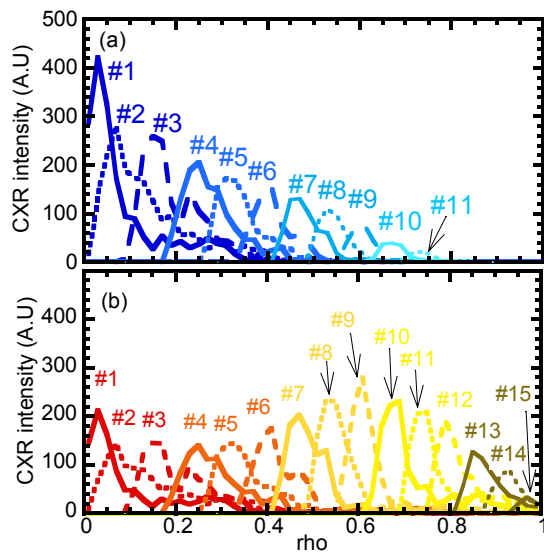


Fig.6 CXR emissivity of the viewing chords for core CXRS measurement in the case of (a) peaked and (b) hollow impurity density profiles.

### 3. References

- [1] F. Wagner *et al.*, Phys. Rev. Lett. **49**, 1408 (1982).
- [2] K.C. Shaing and E.C. Crume, Phys. Rev. Lett. **63**, 2369 (1989).
- [3] K. Ida *et al.*, Phys. Rev. Lett. **65**, 1364 (1990).
- [4] Y. Koide *et al.*, Phys. Rev. Lett. **72**, 3662 (1994).
- [5] T.S. Hahm, Phys. Plasmas **1**, 2940 (1994).
- [6] K. Burrell, Phys. Plasmas **4**, 1499 (1997).
- [7] L.-J. Zheng, M. Kotschenreuther and M.S. Chu, Phys. Rev. Lett. **95**, 255003 (2005).
- [8] Y. Sakamoto *et al.*, Plasma Phys. Control. Fusion **46**, A299 (2004).
- [9] R. J. Fonck, D. S. Darrow, and K. P. Jaehnig, Phys. Rev. A **29**, 3288 (1984).
- [10] S. Nishimura *et al.*, Plasma Fusion Res. **2**, 037 (2007).
- [11] F. Sano *et al.*, Nucl. Fusion **45**, 1557 (2005).
- [12] S. Murakami *et al.*, Trans. Fusion Tech. **27**, 259 (1995).
- [13] S. Kado, private communication
- [14] S. Kobayashi, *et al.*, IAEA-CN-165/EX/P5-13 (2008).